Theoretical study of the spectroscopic and conducting properties of 4,4'-bipyridine and its protonated and reduced species

ARTICLE *in* JOURNAL OF MOLECULAR STRUCTURE THEOCHEM · NOVEMBER 1993

Impact Factor: 1.37 · DOI: 10.1016/0166-1280(93)87228-6

3 AUTHORS, INCLUDING:

Reinaldo Pis Diez
National Scientific and Technical Rese…
93 PUBLICATIONS **530** CITATIONS
SEE PROFILE

Emilce Ottavianelli
National University of Salta
16 PUBLICATIONS **34** CITATIONS
SEE PROFILE

Journal of Molecular Structure (Theochem), 287 (1993) 241–247
0166-1280/93/$06.00

Theoretical study of the spectroscopic and conducting properties of 4,4′-bipyridine and its protonated and reduced species

Reinaldo Pis Diez[a], Alicia H. Jubert*[,a], Emilce Ottavianelli[b]

[a]*Programa QUINOR, Facultad de Ciencias Exactas, UNLP, C.C.962, 1900 La Plata, Argentina*
[b]*Facultad de Ciencias Exactas, Universidad Nacional de Salta, Buenos Aires 177, 4400 Salta, Argentina*

(Received 12 October 1992; accepted 9 March 1993)

Abstract

MNDO calculations were performed on normal and protonated species of 4,4′-bipyridine and its reduced forms. By considering these results, the energetics, geometries, bond orders and wavenumber shifts of several A_g fundamental modes are related and the conducting properties of these species adsorbed on electrodes, as determined by surface-enhanced Raman scattering (SERS), are explained.

Introduction

The potential application of modified electrodes in fields as diverse as sensor design [1,2], energy conversion [3], corrosion protection [4] and catalysis has led to extensive investigations in the area of contemporary electrochemistry.

The nature of charge transport through the modifying layer is recognized as being of central importance, not only for fundamental reasons but also because the applications of these materials are determined by the film's charge transfer transport properties.

Metallopolymers containing covalently bound immobilized redox centers are becoming increasingly recognized as having those properties most desirable for useful applications. One of these properties is the easy electron self-exchange process [5].

In this framework, the ability of 4,4′-bipyridine (Bpy) adsorbed on metal electrodes to enhance redox reactions of certain biological molecules has generated considerable interest [6].

* Corresponding author.

The basis of the surface acceleration is not well known. To obtain information concerning the mechanism, in situ surface spectroscopy such as surface-enhanced Raman scattering (SERS) has previously been performed [7–9]. Considerable attention has been paid to the adsorptive behavior of Bpy because the orientation of the adsorbed molecule is important in accelerating redox reactions at the electrodes [6].

Spectroscopic studies of the various redox forms of Bpy have previously been made and the various species characterized [10,11].

In order to study the charge transport properties of Bpy, semiempirical MNDO calculations have been performed on normal and protonated Bpy and its reduced forms. By considering these results, the energetics, geometries, bond orders and wavenumber shifts of several A_g in-plane fundamental modes have been reported.

Computational details

Calculations have been carried out by the MNDO technique [12] for the various protonated

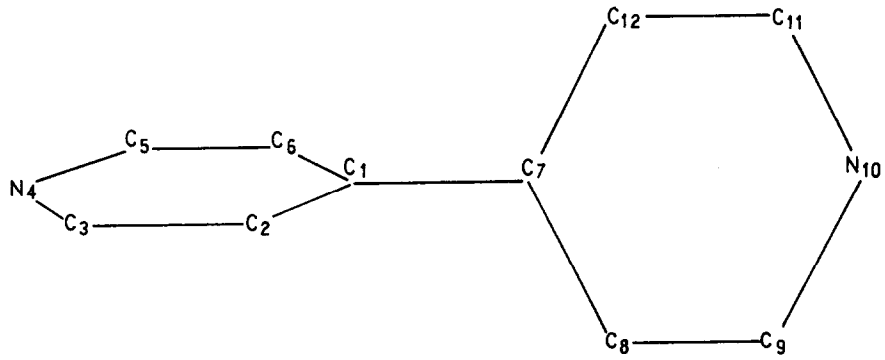

Fig. 1. Structure and numbering of the atoms in 4,4′-bipyridine.

and non-protonated species, employing the original parameterization. The starting geometrical parameters were taken from Ref. 13. All geometrical parameters were optimized as usual by the Davidon–Fletcher–Powell algorithm [14].

Figure 1 shows the structure and numbering of the atoms of 4,4′-bipyridine.

Results and discussion

The ordering and energies of selected occupied and virtual orbitals and their relative positions can be analyzed. Consideration here is restricted to half the molecule because both parts are equivalent.

The HOMO in Bpy is fundamentally π bonding between C_2C_3 and C_5C_6. The HOMO in $Bpy^{\cdot -}$ has π bonding character between C_1C_2 and C_1C_6, π antibonding character between C_1C_7 and $n\pi$ character on the nitrogen atom. In Bpy^{2-} the HOMO is mainly π bonding on C_1C_7, antibonding between C_1C_2 and C_1C_6 and $n\pi$ on the nitrogen atom.

The LUMO on the Bpy is weakly π bonding between C_2C_3 and C_5C_6, antibonding between C_1C_7 and $n\pi$ on the nitrogen atom. In $Bpy^{\cdot -}$ the LUMO has π bonding character on C_1C_7, π antibonding between C_1C_2 and C_1C_6, and $n\pi$ on the nitrogen atom. In Bpy^{2-} the LUMO is π antibonding between C_2C_3 and C_5C_6.

Considering the protonated species $BpyH_2^{2+}$, $BpyH_2^{\cdot +}$ and $BpyH_2$, the HOMOs are: π bonding between C_2C_3 and C_5C_6; π bonding between C_1C_2 and C_1C_6, $n\pi$ on the nitrogen atom and π antibonding on C_1C_7; π bonding between C_1C_7, C_2C_3, C_5C_6 and $n\pi$ on the nitrogen atom, respectively. The LUMOs are mainly: non-bonding on C_1C_7, π antibonding between C_3N_4 and N_4C_5; π bonding between C_2C_3, C_5C_6 and C_1C_7, and $n\pi$ on the nitrogen atom, π antibonding on C_1C_7 and $n\pi$ on C_3C_5, for the three species, respectively.

Considering the eigenvalues, as the negative charge of the species increases from the neutral molecule to $Bpy^{\cdot -}$ and Bpy^{2-}, the energy of the HOMO increases by 4.9 and 12.4 eV, respectively. An increase of 4.3 and 16.2 eV above the $BpyH_2^{2+}$ HOMO is found for the HOMO of the $BpyH_2^{\cdot +}$ and $BpyH_2$ species, respectively. The energy of the LUMO increases by 1.2 and 9.3 eV and 1.2 and 8.9 eV on going from Bpy to $Bpy^{\cdot -}$ and Bpy^{2-}, and from $BpyH_2$ to $BpyH_2^{\cdot +}$ and $BpyH_2$, respectively.

The optimized geometries and the definition of the internal coordinates for the neutral molecule and the protonated and reduced forms of both species are summarized in Table 1.

The geometrical parameters are compared within two different groups: unprotonated species Bpy, $Bpy^{\cdot -}$ and Bpy^{2-}; protonated species $BpyH_2^{2+}$, $PbyH_2^{\cdot +}$ and $BpyH_2$.

Considering the unprotonated species, the C_1C_2, C_3N_4, N_4C_5 and C_6C_1 bond lengths increase together with the negative charge of the compound while the C_2C_3, C_5C_6 and C_1C_7 bond lengths decrease. The CCC and CCN bond angles increase on going from Bpy to Bpy^{2-} while the

Table 1
MNDO optimized geometrical parameters for 4,4′-bipyridine, and its protonated and reduced species[a]

Internal coordinate	Bpy	$Bpy^{\cdot -}$	Bpy^{2-}	$BpyH_2^{2+}$	$BpyH_2^{\cdot +}$	$BpyH_2$
Bond length (Å)						
C_1C_2	1.41	1.44	1.48	1.42	1.44	1.48
C_2C_3	1.42	1.39	1.38	1.41	1.39	1.36
C_3C_4	1.35	1.36	1.37	1.37	1.39	1.40
N_4C_5	1.35	1.36	1.37	1.37	1.38	1.40
C_5C_6	1.41	1.39	1.37	1.41	1.38	1.36
C_6C_1	1.41	1.39	1.37	1.41	1.38	1.36
C_7C_1	1.49	1.44	1.39	1.49	1.45	1.38
Bond angle (deg)						
$C_3C_2C_1$	119.72	121.56	122.51	120.24	121.54	123.61
$C_4C_3C_2$	122.38	123.19	124.99	119.63	119.28	120.47
$C_5N_4C_3$	118.29	116.69	114.23	121.98	121.46	118.96
$C_6C_5C_4$	123.11	124.22	125.80	119.56	120.41	121.77
$C_7C_1C_2$	121.38	123.28	124.78	121.18	121.94	123.71
Torsion angle (deg)						
$N_4C_3C_2C_1$	−0.02	−0.25	0.00	0.01	0.00	−1.54
$C_5N_4C_3C_2$	0.01	0.61	0.13	0.07	0.07	5.32
$C_6C_5N_4C_3$	0.01	−0.37	−0.02	−0.08	−0.08	−6.30
$C_7C_1C_2C_3$	180.15	179.49	179.74	179.96	179.96	178.51
$C_8C_7C_1C_2$	90.53	154.57	178.54	90.50	148.17	178.49

[a] See Fig. 1. for atom numbering.

CNC bond angle decreases, showing the opposite behavior.

The other geometrical parameters do not show any remarkable changes, except for the torsion angle $C_8C_7C_1C_2$, which changes from 90.5° in the neutral molecule to 154.6° in $Bpy^{\cdot -}$ and 178.5° in Bpy^{2-}. The same variational trend in the geometrical parameters is observed within the protonated species.

The change in the bond orders on going from the parent to the reduced species obtained from MO calculations is shown in Table 2. The results suggest a quinonoid structure for Bpy^{2-} through the reinforcement of the C_2C_3, C_5C_6 and C_1C_7 bonds. A structure similar to that of the methyl viologen (1,1′-dimethyl-4,4′-bipyridinium (MV^{2+})) [15] is suggested for the reduced species; the fundamental change in the geometry is the coplanarity of the

Table 2
Bond orders of the non-protonated, protonated and reduced species of 4,4′-bipyridine[a]

Bond	Bpy	$Bpy^{\cdot -}$	Bpy^{2-}	$BpyH_2^{2+}$	$BpyH_2^{\cdot +}$	$BpyH_2$
C_1C_2	0.42	0.23	0.01	0.39	0.22	0.00
C_2C_3	−0.22	−0.11	0.04	−0.15	−0.02	0.09
C_3N_4	0.93	0.77	0.62	0.94	0.81	0.60
N_4C_5	0.07	0.02	−0.06	0.34	0.22	−0.05
C_5C_6	−0.20	−0.11	0.02	−0.11	0.02	0.20
C_6C_1	−0.99	−0.76	0.48	1.01	0.80	0.53
C_1C_7	−0.82	−0.41	0.04	−0.82	−0.53	0.13

[a] See Fig. 1 for atom numbering.

rings, whereas in the neutral molecule they are perpendicular to each other.

Normal Raman (NR) and resonance Raman (RR) studies of the various redox forms of Bpy in aqueous solutions have been performed by Lu et al. [6]. Gupta [10] and Kihara and Gondo [11] have reported the NR spectrum of Bpy in the solid state. The latter authors have also studied the RR spectra of the Bpy radical anion $Bpy^{\cdot -}$ in the solid state and in an organic solvent.

Values of the vibrational models, showing significant changes with the charge of the species within non-protonated and protonated groups of molecules, are summarized in Table 3. These modes are, in the protonated species, well characterized by comparison with MV^{2+}, $MV^{\cdot +}$ and MV^0. For MV^{2+} a normal coordinate analysis of the vibrational modes has been performed [16]. Results in that work indicate that the substituents do not markedly affect the overall symmetry of the molecules or their electronic density.

Bands at 1652 and 1538 cm^{-1} in MV^{2+} are assigned as A_g modes: fundamentally CC and CC, CN ring stretching modes, respectively. The trend within the series for the values of these modes can be explained by inspection of the variation in the bond orders. The highest value for the CN ring stretching mode in $BpyH_2^{2+}$ is consistent with a large contribution of the charge density on the CN bonds in the corresponding LUMOs.

It is commonly agreed that the 1301 cm^{-1} band in MV^{2+} is primarily due to the inter-ring C–C vibration (14% C_2C_3, 30% C_1C_7, 20% δHC_2C_3) and upon reduction to $MV^{\cdot +}$ considerable electron density is added to the C_1C_7 bond, so the frequency shifts to about 1358 cm^{-1} (12% C_2C_3, 32% C_1C_7, 10% δHC_1C_2, 23% HC_2C_3) [16–23]. It is obvious that the previous explanation is not consistent with the potential energy distribution (PED) because only a 2% variation is observed in the contribution to the stretching mode C_1C_7, but a large change is observed in bending contributions to this mode. The same holds for this mode in MV^0, located at 1407 cm^{-1} (14% C_2C_3, 33% C_1C_7, 25% δHC_2C_3, 13% δHC_2C_1). This mode is located at 1298 cm^{-1} in $BpyH_2^{2+}$, and upon reduction changes to 1353 and 1392 cm^{-1} in $BpyH_2^{\cdot +}$ and $BpyH_2$, respectively. This trend can be explained by considering the bond orders of the internal coordinates involved in this mode. It can be seen that the highest contribution is due to the C_2C_3 and C_1C_7 bonds, which show a reinforcement upon the reduction of the species.

The band at 1234 cm^{-1} in MV^{2+} is assigned as a deformation mode δHCC (18% δHC_2C_1, 41% δHC_2C_3, 25% δHC_3N_4), which upon reduction moves to 1252 cm^{-1} (17% δHC_2C_1, 40% δHC_2C_3, 17% δHC_3N_4) and 1290 cm^{-1} (16% δHC_2C_1, 36% δHC_2C_3, 13% δHC_3N_4). It may be seen that the band is sensitive to the nitrogen

Table 3
Raman data for the A_g modes in 4,4′-bipyridine and its protonated and reduced forms (cm^{-1}).

Species[a]			$BpyH_2^{2+}$	$BpyH_2^{\cdot +}$	$BpyH_2$	Bpy	$Bpy^{\cdot -}$
MV^{2+}	$MV^{\cdot +}$	MV^0					
1652	1663	1661	1652	1653	1652	1605	1612
1538	1536	1542	1531	1523	1538	1510	1509
1301	1358	1407	1298	1353	1392	1298	1350
			1256	1236	1291		
1234	1252	1290	1220	1213	1219	1220	1230
1061	1029	996	1072	1043	997	–	1043
			1013	999		1000	990
841	898	810	760	741	749	753	742
660	685	663	644				

[a] Methyl viologen and its reduced species.

substituent because in $BpyH_2^{2+}$ it is split into two bands at 1256 and 1220 cm^{-1}, which upon reduction goes to 1236, 1213 cm^{-1} and 1291, 1219 cm^{-1} in $BpyH_2^{\cdot+}$ and $BpyH_2$, respectively.

The major contribution to these modes involves the C_2C_3 and C_8C_9 bonds, so an increase in the frequency value must be expected because a reinforcement of them is seen through the bond orders.

The band near 1061 cm^{-1} in the MV^{2+} spectrum (20% C_1C_2, 27% C_3N_4, 12% δHC_2C_1, 12% $\delta C_1C_2C_3$, 16% $\delta N_4C_3C_2$) was assigned to the ring breathing vibration. It shifts to 1029 cm^{-1} in $MV^{\cdot+}$ (23% C_1C_2, 28% C_3N_4, 13% δHC_2C_1, 13% $\delta C_1C_2C_3$) and to about 996 cm^{-1} in MV^0 (27% C_1C_2, 25% C_3N_4, 14% δHC_2C_1, 11% $\delta C_1C_2C_3$).

The downward shift in frequency is consistent with the theoretical calculation of electron density for biphenyl, which indicates that the LUMO has a number of nodes that cross several ring C–C bonds. Thus, the addition of an electron to this orbital would result in a weakening of these bonds and consequently a decrease in their vibrational frequency [24].

This ring breathing mode in the spectra of $BpyH_2^{2+}$ and $BpyH_2^{\cdot+}$ splits into two components at 1072, 1013 cm^{-1} and 1042, 999 cm^{-1}, respectively, whereas in $BpyH_2$ is located at 997 cm^{-1}. The frequency shift can be explained by the loosening of the C_1C_2 and C_3N_4 bonds, which is responsible for the major contribution to the normal mode, as can be seen from the bond order variation.

The band at 841 cm^{-1} in MV^{+2} (33% C_1C_2, 24% C_3N_4, 13% N_4CH_3) moves to 898 cm^{-1} (29% C_1C_2, 36% C_3N_4) and 810 cm^{-1} (26% C_1C_2, 43% C_3N_4) in $MV^{\cdot+}$ and MV^0, respectively, with a significant increase in the contribution of the CN bonds to the normal mode upon the reduction of the species.

The decrease of the bond order for the CN bond on going from $BpyH_2^{2+}$ to $BpyH_2^{\cdot+}$ and $BpyH_2$ species justifies the variational trend of the values 760, 741 and 749 cm^{-1} found for these species, respectively, which are assigned as modes with major contributions from the CC and CN stretchings.

The band at 644 cm^{-1} in $BpyH_2^{2+}$ correlates well with the band assigned as the N–CH_3 stretching mode in MV^{2+}. No bands are observed for this mode in the reduced species.

We are now going to analyze the vibrational spectra of the non-protonated species, fundamentally the A_g symmetry modes for Bpy and $Bpy^{\cdot-}$.

To our knowledge, only Gupta [10], and Kihara and Gondo [11] have reported the NR spectrum of Bpy in the solid state. The latter authors also studied the RR spectra of $Bpy^{\cdot-}$ in the solid state and in an organic solvent, and performed normal coordinate analysis and MO calculations (semiempirical Pariser–Parr–Pople) on neutral Bpy and the Bpy radical anion. Unfortunately, they took the geometry of $Bpy^{\cdot-}$ to be the same as that of neutral Bpy, which is not so, as we have proved through our calculations, which makes their conclusions doubtful.

The band at 1605 cm^{-1} in Bpy can be correlated with the mode with a major contribution (54%) from the ν_{CC} of the ring in biphenyl [25] (1612 cm^{-1}) and that at 1581 cm^{-1} in liquid pyridine [26]. The band is located at 1612 cm^{-1} in $Bpy^{\cdot-}$. By inspection of the bond order changes one can conclude that a large contribution of the quinonoid structure must be considered in order to justify the shift in the mode.

The band at 1510 and 1509 cm^{-1} in Bpy and $Bpy^{\cdot-}$, respectively, correlates with that at 1507 cm^{-1} in biphenyl [25] assigned fundamentally as a ν_{CC} of the ring (33%) and an inter-ring ν_{CC} (26%), and with that at 1481 cm^{-1} of a_1 type in pyridine [26]. The same value in both species can be explained by a compensation effect between reinforcement and loosening of the bonds involved in the normal mode.

The 1350 cm^{-1} band of $Bpy^{\cdot-}$, the pivot-bond stretching band, shows an upward shift of 52 cm^{-1} compared with the corresponding band for neutral Bpy [11]. The upward shift is larger than that of 39 cm^{-1} found for the biphenyl radical anion [25] when compared with neutral biphenyl; the shifts in

the other bands are smaller than those for the biphenyl radical anion. Similar upward shifts have also been found in the 2,2′-Bpy radical anion [26].

The bond order changes on going from the parent molecule to the corresponding radical, as obtained from the MO calculations, suggest a quinonoid structure for $Bpy^{\cdot -}$, supporting the frequency shift given in Table 3. Similar quinonoid structures have been found in the 2,2′-Bpy radical anion and the methyl viologen radical cation [27,28].

It can also be proved that replacing the CH groups by nitrogen atoms makes the structure tend to be more quinonoidal in $Bpy^{\cdot -}$ than in the biphenyl radical anion [25].

The band at $1220\,cm^{-1}$ in neutral Bpy can be correlated with that at $1281\,cm^{-1}$ in biphenyl [29], fundamentally a ν_{CC} of the ring, and with that of species a_1 at $1218\,cm^{-1}$ in pyridine [30].

By inspection of the bond order variation, the reinforcement in some CC bond lengths is clearly compensated by the loosening of other CC bond lengths in the same ring and almost no variation must be expected in the position of this mode upon the reduction of the species.

The Raman band of neutral Bpy corresponding to the $1043\,cm^{-1}$ band of $Bpy^{\cdot -}$ is apparently too weak to be observed, whereas the ring breathing mode at $1000\,cm^{-1}$ in neutral Bpy appears as a very strong band, which upon reduction changes to $990\,cm^{-1}$ in $Bpy^{\cdot -}$. This mode correlates with that at $996\,cm^{-1}$ in biphenyl [29] and $989\,cm^{-1}$ in pyridine [30] (a_1).

The band at $753\,cm^{-1}$ in neutral Bpy changes to $742\,cm^{-1}$ in $Bpy^{\cdot -}$ and correlates with the band at $737\,cm^{-1}$ in biphenyl [29], fundamentally ν_{CC} of the ring and δ_{HCC}.

Conclusions

Results of semiempirical calculations on the protonated, non-protonated and reduced species derived from 4,4′-bipyridine show that significant geometrical and electronic density changes occur upon reduction of Bpy and $BpyH_2^{2+}$.

The C–C inter-ring bond gains partial double bond character in the reduced species. Some electronic delocalization is observed between the two pyridyl rings, which are likely to be stabilized under a coplanar conformation in the reduced species.

This characteristic seems to be responsible for the conducting properties of Bpy upon reduction and the shift in several A_g normal modes of the adsorbed species upon reduction, as observed in the SERS spectra. Nevertheless, the first assumption has not been confirmed experimentally because bipyridines appear to accelerate the rate of heterogeneous electron transfer processes by a non-mediation mechanism, because these compounds are electro-inactive at the working potential [9].

References

1 R.W. Murray, in A.J. Bard (Ed.), Electroanalytical Chemistry, Vol. 13, Marcel Dekker, New York, 1983, p. 191.
2 W.J. Aberyand and A.R. Hillman, Annu. Rep. Prog. Chem., Sect. C, (1981) 377.
3 P.V. Kamat, M.A. Fox and A.J. Fatiadi, J. Am. Chem. Soc., 106 (1944) 1191.
4 T. Ohsawa, K. Kaneko and K. Yoshino, Jpn. J. Appl. Phys., 23 (1984) L663.
5 A.R. Hillma, in R.E. Linford (Ed.), Electrochemical Science and Technology of Polymers, Vol. 1, Elsevier, Amsterdam, 1987, Chapter 5, p. 103.
6 T. Lu, T.M. Cotton, R.L. Birke and J.R. Lombardi, Langmuir, 5 (1989) 404, and references cited therein.
7 T.M. Cotton, D. Kaddi and D. Iorga, J. Am. Chem. Soc., 105 (1983) 7462.
8 T.M. Cotton and M. Vavra, Chem. Phys. Lett., 106 (1984) 491.
9 I. Taniguchi, M. Iseki, H. Yamaguchi and K. Yasukouchi, J. Electroanal. Chem., 186 (1985) 299.
10 V.P. Gupta, Ind. J. Pure Appl. Phys., 11 (1973) 775.
11 H. Kihara and Y. Gondo, J. Raman Spectrosc., 17 (1986) 263.
12 M.J.S. Dewar and W.J. Thiel, J. Am. Chem. Soc., 99 (1977) 4899, 4907; M.J.S. Dewar and H.S. Rupa, J. Am. Chem. Soc., 100 (1978) 777.
13 L.E. Sutton (Ed.), Tables of interatomic distances and configuration in molecules and ions, Special Publication No. 11, The Chemical Society, London, 1958.
14 R. Fletcher and M.I.D. Powell, Comput. J., 6 (1963) 163; W.C. Davidon, Comput. J., 10 (1968) 406.

15 S. Goshal, T. Lu, Q. Feng and T.M. Cotton, Spectrochim. Acta, Part A, 44 (1988) 651, and references cited therein.
16 P.C. Lee, K. Schmidt, S. Gordon and D. Meisel, Chem. Phys. Lett., 80 (1981) 242.
17 A. Regis and J. Corset, J. Chim. Phys., 78 (1981) 647.
18 M. Forster, R.B. Girling and R.E. Hester, J. Raman Spectrosc., 12 (1982) 36.
19 R.E. Hester and S. Suzuki, J. Phys. Chem., 86 (1982) 4626.
20 O. Poizat, C. Soorisseal and Y. Mathey, J. Chem. Soc., Faraday Trans. 1, 80 (1984) 3257.
21 Q. Feng and T.M. Cotton, J. Phys. Chem., 90 (1986) 983.
22 T. Lu, L. Birke and J.R. Lombardi, Langmuir, 2 (1986) 305.
23 M. Datta, R.E. Jabsson and J.J. Freeman, Appl. Spectrosc., 40 (1986) 251.
24 M.J.S. Dewar and N. Trinajstic, Collect. Czech. Chem. Commun., 35 (1970) 3136.
25 S. Yamaguchi, J. Yoshizumi and S. Maeda, J. Phys. Chem., 82 (1978) 1078.
26 R.F. Darlinger and W.H. Woodruff, J. Am. Chem. Soc., 101 (1978) 4391.
27 M. Forster and R.E. Hester, Chem. Phys. Lett., 81 (1981) 42.
28 R.E. Hester and S. Suzuki, J. Phys. Chem., 86 (1982) 4626.
29 G. Zerbi and S. Sandroni, Spectrochim. Acta, Part A, 24 (1968) 483.
30 R.K. Chang and T.E. Furtak (Eds.), Surface Enhanced Raman Scattering, Plenum, New York, 1982.